symmetry

MDPI

Article

A Kinetic BGK Model for Pedestrian Dynamics Accounting for Anxiety Conditions †

Nouamane Bakhdil [1,*], Abdelghani El Mousaoui [2] and Abdelilah Hakim [1]

[1] Laboratory of Applied Mathematics and Computer Science, Faculty of Sciences and Technologies of Marrakech, Cadi Ayyad University, Marrakech 40000, Morocco; a.hakim@uca.ma
[2] School of Industrial Management, Mohammed VI Polytechnic University, Ben Guerir 43150, Morocco; abdelghani.elmousaoui@emines.um6p.ma
* Correspondence: nouamane.bakhdil@ced.uca.ma
† Dedicated to the memory of Abdelghani Bellouquid.

Abstract: This article presents a kinetic model based on the BGK equation to simulate pedestrian dynamics, with a specific focus on anxiety conditions. The proposed model is based on the idea that for pedestrians in equilibrium, where this term is used to indicate that the system is characterized by a symmetric equilibrium velocity distribution with a relaxation term, the anxiety factor is incorporated into the equilibrium distribution through the preferred velocity, leading to potential symmetry-breaking effects in pedestrian dynamics. In addition, this paper introduces a numerical resolution scheme using the Monte Carlo particle method that effectively captures both symmetric and asymmetric behaviors of pedestrians. This method is applied to simulate crowd evacuation during stressful situations and pedestrian bidirectional flow in a straight corridor.

Keywords: crowd dynamics; kinetic theory; BGK model; Monte Carlo particle method; evacuation time; counter-flow

check for updates

Academic Editor: Nicola Bellomo

Received: 6 December 2024
Revised: 19 December 2024
Accepted: 24 December 2024
Published: 26 December 2024

Citation: Bakhdil, N.; El Mousaoui, A.; Hakim, A. A Kinetic BGK Model for Pedestrian Dynamics Accounting for Anxiety Conditions. *Symmetry* **2025**, *17*, 19. https://doi.org/10.3390/sym17010019

Copyright: © 2024 by the authors. Licensee MDPI, Basel, Switzerland. This article is an open access article distributed under the terms and conditions of the Creative Commons Attribution (CC BY) license (https://creativecommons.org/licenses/by/4.0/).

1. Introduction

The computational modeling and simulation of pedestrian dynamics has garnered significant attention due to the potential benefits in terms of wellbeing and security. For instance, simulations contribute to supporting crisis managers in handling perilous circumstances such as emergency evacuation processes caused by fire, earthquakes, and conflicts with antagonist groups [1].

The proposed models of pedestrian dynamics can be grouped into three categories based on scale. One category is the *microscopic* model, which is individual-based and inspired by Newtonian mechanics, focusing on inter-particle interactions. The social force model (SFM) [2] and cellular automata model [3] are also prominent microscopic models.

The second category views pedestrian dynamics as a continuum of flow, an approach that is particularly effective for large-scale dense crowds. The primary reference for macroscale models is the book [4]; see Aylaj et al. [5] for a unified framework that provides a consistent multiscale description of human crowd models at the macroscopic, mesoscopic, and microscopic levels.

The third category, known as the *mesoscopic* or kinetic model, uses an observational scale between the two previously mentioned. Within this framework, pedestrians are modeled as *active particles*, with their microscopic state including mechanical variables such as position and velocity along with an additional variable termed "*activity*" to model the non-mechanical state (e.g., a social state) [6]. The system's overall state is characterized by

a distribution function f over the micro-state. The kinetic theory of active particles, KTAP for short, has thus far been actively used to derive a variety of models of complex living systems, for example, epidemiological models for pandemics [7], vehicular traffic [8] and collective learning [9], which is currently an important topic in artificial intelligence [10]; see the studies outlined in [11], which explore the theory of the artificial world in light of the visionary philosophy of Herbert A. Simon [12]. In this paper, we select a kinetic-based model due to its adaptability in modeling various interactions and heterogeneous pedestrian behavior [1,13,14].

Bellomo et al. initiated the study of kinetic models of human crowds [15,16]. Subsequent research further developed these models to capture crowd dynamics within bounded environments, including interactions with walls, exits, and obstacles [17–20]. One such model considers a leader–follower system in crowd evacuation with collective learning [21], while another introduces factors such as visual attention to analyze congestion in long-distance passages [22]. Recent research has been dedicated to understanding the behavioral and social dynamics of crowds. For example, a kinetic model was developed to simulate crowd dynamics, considering stress conditions, boundary conditions, and safety concerns [23,24]. Bellomo et al. also investigated emergent behaviors in crowds, emphasizing the impact of emotional states on overall crowd dynamics [1,6,25,26]. In a related study, a 2D mesoscopic model was developed to model the dynamics of heterogeneous social groups in a crowd moving in a domain with boundaries and outlet doors [27]. Additionally, an extension of a kinetic model for crowd evacuation from bounded domains was presented to address the spread of an infectious respiratory disease within indoor venues [28,29]. In light of the global COVID-19 crisis, the contributions in [30,31] studied the initial transmission of highly infectious diseases through social interaction using the integration of a kinetic pedestrian dynamics model with a contagious disease model. A data-driven learning was used in [32] to improve a kinetic model of pedestrian dynamics in distress by incorporating stress as a parameter and estimating it through an inverse crowd dynamics problem, with preliminary results based on synthetic data where the stress level is clearly defined [32].

A number of previously cited works have employed mathematical frameworks to derive models at the mesoscopic scale, which are expressed through an evolution equation for the distribution function f. The fundamental structure of this equation is as follows:

$$\partial_t f(t, \boldsymbol{x}, \boldsymbol{v}) + \boldsymbol{v} \cdot \nabla_{\boldsymbol{x}} f(t, \boldsymbol{x}, \boldsymbol{v}) = J[f, f](t, \boldsymbol{x}, \boldsymbol{v}), \tag{1}$$

where $\boldsymbol{x}$ is the position of each walker, $\boldsymbol{v}$ is the velocity of each pedestrian, and the operator $J[f, f]$ characterizes the different nonlinear interactions between pedestrians and their environment, such as walls and obstacles.

The nonlinear integro-differential nature of the kinetic Equation (1) leads to a computationally complicated model. The computational cost can be significantly reduced if the mathematical structure (1) is simplified.

In this work, we expand our kinetic-type model presented in [33] to incorporate pedestrian behavior, specifically addressing anxiety conditions. The model's key components are as follows. (i) it provides a straightforward method for modeling the interactions term $J[f, f]$ of the kinetic Equation (1), akin to the Bhatnagar–Gross–Krook (BGK) operator, which replaces the Boltzmann equation's collision operator [33]. This component describes pedestrians' inclination towards an equilibrium state. (ii) It operates under the assumption that pedestrians are in an equilibrium, where this term denotes that the entire system is characterized by a equilibrium velocity distribution with a relaxation time [34]. (iii) The equilibrium velocity distribution is established through an analysis of pedestrian velocity distributions under various conditions from previous studies [33,35].

Our model aims to replicate pedestrian movement towards a particular destination while maximizing comfort. For instance, during evacuations pedestrians aim to attain a preferred velocity in order to reach an exit efficiently. Incorporation of the anxiety factor into the equilibrium distribution is achieved through the preferred velocity. This preferred velocity is pivotal, and significantly impacts the model's effectiveness. It considers a range of factors influencing walking behavior, encompassing *rational actions* such as the urge to reach an exit, navigating obstacles or walls, and avoiding crowded areas, as well as *irrational behaviors* such as being drawn to the main flow due to heightened anxiety levels. Numerical simulations employing the Monte Carlo particle method [27,36] have been developed to examine the effect of anxiety levels on evacuation duration and explore pedestrian counter-flows in a straight corridor.

The rest of this article is structured as follows: Section 2 introduces the mathematical BGK model of pedestrian dynamics; Section 3 is devoted to modeling the preferred velocity in the presence and the absence of walls and obstacles and with the consideration of the anxiety factor; Section 4 briefly describes the Monte Carlo particle method, then presents simulation results in order to examine the predictive ability of the suggested model to support crisis managers; finally, our conclusions are provided in Section 5.

2. The Kinetic BGK Model for Pedestrian Dynamics

The quest for a mathematical theory of living systems is a profound scientific challenge of this century. Traditional approaches rooted in conservation or equilibrium equations of inert matter are insufficient for describing the unique dynamics of living systems, which are, as **Immanuel Kant (1724–1804)** observed, *special structures organized and with the ability to chase a purpose* [37].

Erwin Schrödinger (1887–1961) looked for a physical theory in which cells modify their state due to interactions with other cells [38]. His pioneering ideas chased a systems approach motivated by the study of mutations, including those induced by external factors such as radiation. He proposed that the dynamics at the level of cells are driven by the dynamics at the molecular scale, a concept that remains crucial in understanding the interactions between mathematics and biology [14]. The ability of living systems to extract entropy to maintain low levels highlights their strategy, introducing the concept of active particles [14,38].

Nobel laureate **Lee Hartwell (born 1938)** further emphasized that biological systems fundamentally differ from inanimate matter, pointing to their inherent functionality and purpose [39]. He argued that while living systems obey physical and chemical laws, their dynamics cannot be straightforwardly described using the mathematics of inert matter. Instead, they require innovative modeling strategies that reflect the complexity and organization inherent in living matter [14,39]. These perspectives shape the challenging research pathway toward deriving a mathematical framework capable of addressing the intricate interplay between mathematics and the dynamics of living systems, particularly pedestrian dynamics [1,14].

In the context of pedestrian dynamics, the distinction between living and inert systems is crucial. The dynamics of living particles, such as pedestrians in a crowd, differ significantly from those of inert systems due to their purposeful and adaptive behaviors [1]. Pedestrians act continually, interacting with one another and being influenced by emotions, intentions, and environmental factors [6]. The kinetic theory of active particles offers a powerful framework to model such systems, treating pedestrians as self-propelled particles characterized by heterogeneous abilities and strategies [21,26]. Unlike classical particles that respond sharply upon colliding with a boundary, pedestrians viewed as active particles sense and adapt to their environment, gradually modifying their trajectories in response to

obstacles or interactions with other pedestrians [6]. This nuanced modeling captures the unique behaviors and interactions of living systems, providing a bridge between the mathematics of inert matter and the complexities of purposeful organized dynamics observed in pedestrian flows [40,41].

In particular, traditional kinetic models such as the Bhatnagar–Gross–Krook (BGK) operator, which have been used to describe the behavior of gases [42], provide a useful framework for understanding the collective dynamics of pedestrians [33,34]. However, pedestrian behavior cannot be modeled simply as a series of particles colliding and reaching equilibrium. Instead, these active particles are governed by social interactions, individual goals, and emotional states, all of which complicate the classical notion of equilibrium. When extended to include factors such as anxiety or social influence, the BGK model becomes a tool for capturing not just physical motion but the psychological and social dynamics that shape pedestrian movement.

In this part, we extend the BGK framework to incorporate the notion of equilibrium in the context of pedestrian dynamics, acknowledging that true equilibrium in living systems is a dynamic and adaptive process, not a static state. The key challenge here is reconciling the concept of equilibrium velocity distribution, with the inherently non-equilibrium nature of living systems [43].

In our model, equilibrium is defined not as a state of rest or uniformity but as a tendency towards a comfortable and stable state of motion that pedestrians naturally strive for given certain conditions. This state of equilibrium reflects a balance between pedestrians' individual goals (e.g., reaching a destination) and their social interactions (e.g., avoiding congestion, aligning with others). The relaxation time in the BGK model controls how quickly pedestrians adjust to changes in their environment, which includes interactions with other pedestrians and obstacles as well as anxiety-driven behaviors.

This section presents the mathematical BGK model of behavioral crowd dynamics. The concept of pedestrians in a state of equilibrium is presented first, followed by the mathematical structure, the equilibrium velocity distribution, and the relaxation time.

2.1. Pedestrians in a State of Equilibrium

We consider the dynamics in a two-dimensional domain denoted by Ω within which the crowd moves. The region containing the entire crowd at the initial time is represented by a disk $\Omega_0 \subseteq \Omega$ with radius r. The diameter of the circle containing Ω is denoted by L.

At instant $t = t_0$, the system consists of N pedestrians uniformly distributed within the disk Ω_0. The initial overall density is

$$\rho_0 = \frac{N}{\pi r^2} \quad ped/m^2. \tag{2}$$

This group of N pedestrians is situated in the domain Ω at the initial time t_0. They are in a normal state, which means that they have the possibility of heading in all possible directions. They tend to reach a state of equilibrium within a certain time of relaxation, that is, the tendency towards a comfortable situation. For example, if a pedestrian's motion is not disturbed, he/she will walk at the desired velocity; indeed, in a state of equilibrium, all pedestrians aim to reach a "comfortable" destination represented by v^p. The group of pedestrians exhibits a tendency to reach a target (an exit) positioned at the point x_C [33].

2.2. Variables and Parameters of the Proposed Model

As in [1], we introduce the parameter $\alpha \in [0, 1]$ which models the overall quality of the venue, where:

- $\alpha = 1$ reflects high environmental quality.

- $\alpha = 0$ corresponds to low environmental quality.

Polar coordinates are considered for the velocity variable, namely, $\boldsymbol{v} = \{v, \theta\}$, where v represents the speed and θ corresponds to the direction of velocity.

We define the space of velocity such that $\mathcal{V} = \{(v, \theta) : 0 \leq v \leq V_m \text{ and } \theta \in [0\, 2\pi)\}$, where V_m is the maximum speed that a fast pedestrian can achieve in free-flow conditions [1].

Remark 1. *Dimensionless quantities are utilized by referring all speeds to the maximum velocity V_m, all linear space components to a characteristic length L, and dividing time t by the real time T_r determined by the ratio between L and V_m. Therefore, the values of all practical quantities range between* $[0, 1]$.

The mesoscopic description of the overall system is delivered by the statistical distribution $f(t, \boldsymbol{x}, \boldsymbol{v})$ at time t over the micro-state.

If f is locally integrable, then $f(t, \boldsymbol{x}, \boldsymbol{v})d\boldsymbol{x}d\boldsymbol{v}$ is the expected number of pedestrians at time t whose microscopic state is comprised in the elementary volume $d\boldsymbol{x}d\boldsymbol{v}$ of the phase space centered at $(\boldsymbol{x}, \boldsymbol{v})$. The statistical distributions are normalized by $\rho_{\max}$, which defines the maximal full packing density of pedestrians [1].

Macroscopic quantities can be obtained by velocity-weighted moments of the distribution function. For instance, the density can be expressed as

$$\rho(t, \boldsymbol{x}) = \int_{\mathcal{V}} f(t, \boldsymbol{x}, \boldsymbol{v}) d\boldsymbol{v}, \tag{3}$$

the mean velocity represented by

$$\boldsymbol{\xi}(t, \boldsymbol{x}) = \frac{1}{\rho(t, \boldsymbol{x})} \int_{\mathcal{V}} \boldsymbol{v} f(t, \boldsymbol{x}, \boldsymbol{v}) d\boldsymbol{v}, \tag{4}$$

and the total number of pedestrians N in Ω at time t provided by

$$N(t) = \int_{\Omega} \rho(t, \boldsymbol{x}) d\boldsymbol{x}. \tag{5}$$

2.3. Mathematical Structure

The representation of the system is characterized by an equilibrium velocity distribution $\mathcal{S}_{\text{eq}}$ and a relaxation parameter τ to model the movement of pedestrians who want to reach a preferred velocity $\boldsymbol{v}^p$ [33]. The basic structure reads as follows:

$$\partial_t f(t, \boldsymbol{x}, \boldsymbol{v}) + \boldsymbol{v} \cdot \nabla_{\boldsymbol{x}} f(t, \boldsymbol{x}, \boldsymbol{v}) = \frac{1}{\tau[\rho]} \left(\mathcal{S}_{\text{eq}}(\boldsymbol{v} \to \boldsymbol{v}^p)[\rho] - f(t, \boldsymbol{x}, \boldsymbol{v}) \right) \tag{6}$$

where:

- The coefficient τ expresses that the distribution f does not instantly reach the velocity distribution $\mathcal{S}_{\text{eq}}$, but requires some time, called the relaxation time τ [33]. This term may depend on the density $\rho(t, \boldsymbol{x})$; for simplicity, we assume it to be a constant

$$\tau[\rho] = \tau_0. \tag{7}$$

- The equilibrium density $\mathcal{S}_{\text{eq}}$ models the equilibrium state in which each pedestrian wishes to achieve a preferred velocity $\boldsymbol{v}^p$.

The terms $\mathcal{S}_{\text{eq}}$ and $\boldsymbol{v}^p$ are described in detail in the following.

Remark 2. *It is worth noting that square brackets are used in Equation (6) to indicate the dependence of the equilibrium density $\mathcal{S}_{\text{eq}}$ on the density $\rho(t, \boldsymbol{x})$. Thus, despite its linear appearance, the mathematical structure is strongly nonlinear.*

2.4. Equilibrium Density

Based on [33,35], the equilibrium function $\mathcal{S}_{\text{eq}}$ is associated with pedestrian density and influenced by interactions such as avoidance and deceleration. Thus, the equilibrium velocity distribution $\mathcal{S}_{\text{eq}}$ is a exponential decay, defined as follows:

$$\mathcal{S}_{\text{eq}}(\boldsymbol{v}, \rho) = \frac{\rho(t, \boldsymbol{x})}{2\pi v_m^2} \exp\left(-\frac{1}{2} \frac{\|\boldsymbol{v} - v^p(\cos\theta^p, \sin\theta^p)\|^2}{v_m^2} \right) \tag{8}$$

where:

- The preferred velocity $\boldsymbol{v^p}$ has been decomposed into preferred speed v^p and preferred direction θ^p as $\boldsymbol{v^p} = \{v^p, \theta^p\}$.
- $v_m = \sqrt{\frac{1}{2}\int_{\mathcal{V}} \|\boldsymbol{v}\|^2 f(t, \boldsymbol{x}, \boldsymbol{v}) \mathrm{d}\boldsymbol{v}}$.

Remark 3. *Taking the integral over $\mathcal{V}$ on both sides of Equation (8), we have*

$$\int_{\mathcal{V}} \mathcal{S}_{\text{eq}}(\boldsymbol{v}, \rho) \mathrm{d}\boldsymbol{v} = \int_{\mathcal{V}} \frac{\rho(t, \boldsymbol{x})}{2\pi v_m^2} \exp\left(-\frac{1}{2} \frac{\|\boldsymbol{v} - \boldsymbol{v^p}\|^2}{v_m^2} \right) \mathrm{d}\boldsymbol{v} = \rho(t, \boldsymbol{x}). \tag{9}$$

As a consequence of (9), taking the integral over $\Omega \times \mathcal{V}$ on both sides of Equation (6) shows that the proposed model obeys only the conservation of mass in time [33]:

$$N(t) = \int_{\Omega}\int_{\mathcal{V}} f(t, \boldsymbol{x}, \boldsymbol{v}) d\boldsymbol{v} = \int_{\Omega}\int_{\mathcal{V}} f(0, \boldsymbol{x}, \boldsymbol{v}) d\boldsymbol{v} = N(0). \tag{10}$$

3. Towards the Selection of the Preferred Velocity

This part presents the primary novelty of our work, which lies in the development of the preferred velocity $\boldsymbol{v^p} = \{v^p, \theta^p\}$, which is pivotal as it significantly impacts the model's effectiveness. A significant distinction between our modified model and the previous model in [33] is that $\boldsymbol{v^p} = \{v^p, \theta^p\}$ in the earlier model represented only the desire to attain a defined purpose or meeting point; by integrating the anxiety factor along with rational actions and irrational behaviors, our model more accurately reflects the complex dynamics of pedestrian behavior.

In this context, we draw inspiration from the paper by Bellomo and Gibelli on the mathematical theory of behavioral–social dynamics for pedestrian crowds, which provides a comprehensive framework for understanding the interactions and behaviors of individuals within a crowd through a mathematical lens [25]. Their insights into how social factors and individual behaviors influence crowd dynamics have informed our approach to developing the preferred velocity $\boldsymbol{v^p} = \{v^p, \theta^p\}$.

To streamline the presentation of this section, the following set of equations and other relations are summarized. This approach facilitates a clearer understanding of the key components of the model.

Based on [25,26], the basic assumptions related to determining the preferred velocity $\boldsymbol{v^p} = \{v^p, \theta^p\}$ are as follows:

1. We suppose that the interactions between walkers influence their dynamics in two ways:
   - First, by changing the direction of movement $\theta \to \theta^p$.
   - Second, by modifying their velocity modulus $v \to v^p$.
2. All pedestrians are subject to various stimuli, including (1) rational movement of pedestrians, i.e., the tendency to move towards an exit or meeting point, ability to avoid collisions with walls or obstacles, and desire to avoid overcrowded areas, and

(2) irrational movement of pedestrians induced by the level of anxiety, such as being attracted to the main flow (doing what others do).

3. The selection of the velocity direction $\theta \to \theta^p$ corresponds to a weighted selection of the stimuli mentioned in Item 2, depending on the quality of the venue α, level of anxiety, and the density ρ.
4. Obstacles and walls geometrically change the direction of movement $\theta \to \theta^p$ and induce an additional desire to avoid them.
5. After a walking direction has been selected, each pedestrian adapts their speed $v \to v^p$ to the mean speed $||\boldsymbol{\xi}||$ and density ρ, depending on the parameters of venue quality α and level of anxiety.
6. As in [26], the heuristic modeling of speed dynamics is founded on the following reasoning: *If a walker's speed is less than (greater than) the average speed, they are inclined to increase (decrease) their speed. This is driven by a decision process facilitated by low perceived density and overall quality of the venue.*

This section is dedicated to modeling the preferred velocity $\boldsymbol{v}^p$. We commence by modeling the preferred direction θ^p and then the preferred velocity modulus v^p.

3.1. Selection of the Preferred Direction of Motion

First, referring to [25], we assume that three types of stimuli contribute to the modification of walking direction:

- The desire to attain a defined purpose or a meeting point T, represented by the unit vector

$$\boldsymbol{v}^t = \frac{\boldsymbol{x}_T - \boldsymbol{x}_P}{\|\boldsymbol{x}_T - \boldsymbol{x}_P\|}, \tag{11}$$

  where $\boldsymbol{x}_P$ and $\boldsymbol{x}_T$ are the position of the walker in a point P and T, respectively.

Remark 4. *The unit vector $\boldsymbol{v}^t$ represents the desired direction of movement towards a target (e.g., to reach a nearest exit) or meeting point T. This vector points from the current position P to the target T.*

- The attraction toward the mean stream induced by the other pedestrians, represented by the unit vector

$$\boldsymbol{v}^s = \frac{\boldsymbol{\xi}}{\|\boldsymbol{\xi}\|}, \tag{12}$$

  where $\boldsymbol{\xi}$ is the mean velocity provided by (4) and $\|\boldsymbol{\xi}\|$ is the mean speed.

Remark 5. *The term "attraction toward the mean stream" represented by the unit vector $\boldsymbol{v}^s$ suggests a tendency to align with or move in the direction of the mean flow or average movement of other pedestrians. This term is often referred to as "herding behavior", e.g., the tendency to do what all other walkers do [27].*

- The attempt to avoid congested zones is represented by the unit vector

$$\boldsymbol{v}^v = -\frac{\nabla_{\boldsymbol{x}}\rho}{\|\nabla_{\boldsymbol{x}}\rho\|}, \tag{13}$$

  where ρ is the density provided by (3).

Remark 6. *Therefore, $\boldsymbol{v}^v$ is a unit vector pointing away from the highest density regions, indicating an attempt to avoid congestion by moving toward areas with lower density [27].*

An important new trend in the study of human crowds is the introduction of a behavioral variable representing the specific social–emotional state of pedestrians [1]. Different emotional

behaviors have been studied to understand their ability to affect the overall crowd dynamics [6], including stress emotion [25], the propagation of stress in time and space [26], emotional contagion (fear emotion) [30,31] and learning level of the followers [21]. As in [25], we introduce the parameter $\beta \in [0,1]$ that models the overall anxiety of the crowd, where:

- $\beta = 1$ represents a high level of anxiety.
- $\beta = 0$ represents a minimal level of anxiety.

Remark 7. *For the sake of simplicity, the parameter β is a scalar variable that is equally shared by all pedestrians and is not modified by interactions [6].*

In this part, we begin by modeling the preferred direction θ^p, first in the absence of walls and obstacles and then in their presence.

Case 1: in the absence of walls and obstacles

Referring to [25], at low density, pedestrians tend to move towards the meeting point identified by the unit vector $\boldsymbol{v}^t$ unless their anxiety levels are high, in which case they tend to follow the mean stream, indicated by the unit vector $\boldsymbol{v}^s$. On the other hand, at high density pedestrians try to move away from more congested areas by walking in the direction of $\boldsymbol{v}^v$; consequently, the following preferred direction of velocity is proposed:

$$\boldsymbol{v}^1 = \frac{(1-\rho)\frac{(1-\beta)\boldsymbol{v}^t+\beta\boldsymbol{v}^s}{\|(1-\beta)\boldsymbol{v}^t+\beta\boldsymbol{v}^s\|} + \rho\boldsymbol{v}^v}{\left\|(1-\rho)\frac{(1-\beta)\boldsymbol{v}^t+\beta\boldsymbol{v}^s}{\|(1-\beta)\boldsymbol{v}^t+\beta\boldsymbol{v}^s\|} + \rho\boldsymbol{v}^v\right\|}. \tag{14}$$

The preferred angle of motion θ^1 is obtained from Equation (14) through the relation

$$\boldsymbol{v}^1 = \left(\cos\theta^1, \sin\theta^1\right). \tag{15}$$

Remark 8. *In Equation (14), the level of anxiety β affects the attraction towards the stream with respect to the trend towards the target.*

Case 2: in the presence of walls and obstacle

The decision-making process by which walkers select their desired walking direction is also influenced by the presence of walls and obstacles [25]. Referring to [26], the preferred angle of motion is denoted by θ^p, and is chosen in two stages.

In the first stage, the walker at point P selects the direction θ^1 defined by Equation (15), i.e., $\theta^1 = \theta^p$. If this motion direction leads toward the meeting point T, then θ^1 remains unchanged; see Figure 1.

Otherwise, if the motion direction is pointing towards a point P_w on the boundary, then the direction is adjusted by a weighted choice between θ^1, which is defined by Equation (15) and the direction θ^t of $\boldsymbol{v}^t$, where the weight is determined by the distance between the points P and P_w is provided by $d_w = |P - P_w|$; see Figure 2.

Hence, the preferred angle θ^p of motion in the presence of obstacles and walls reads

$$\theta^p = (1 - d_w)\theta^t + d_w\theta^1, \tag{16}$$

where d_w should be equal to one, i.e., $d_w = 1$ if θ^1 is pointed toward the meeting point T [26].

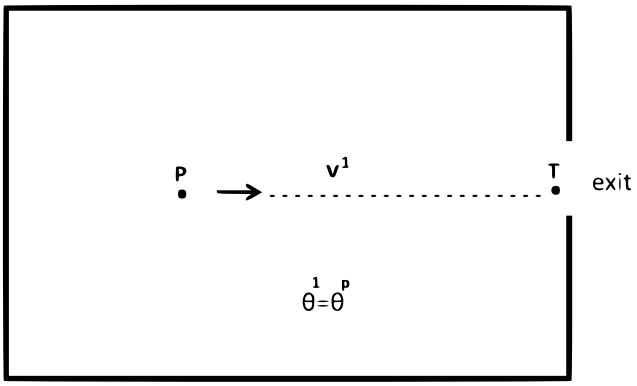


Figure 1. Pedestrian at point P selects the direction θ^1 of velocity v^1 toward the exit point T.

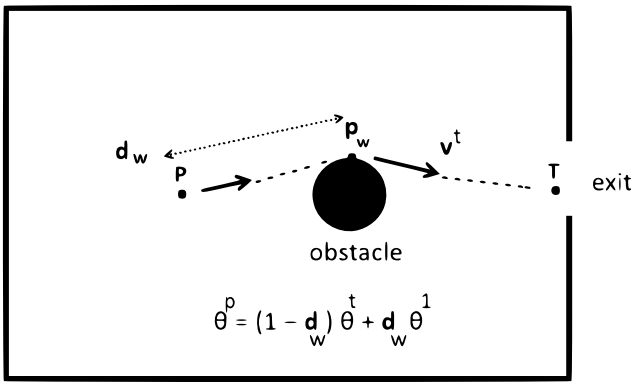


Figure 2. Pedestrian at point P tries to avoid an obstacle in order to reach the exit point T.

The main features involved in selecting the preferred direction θ^p of motion are summarized in Figure 3.

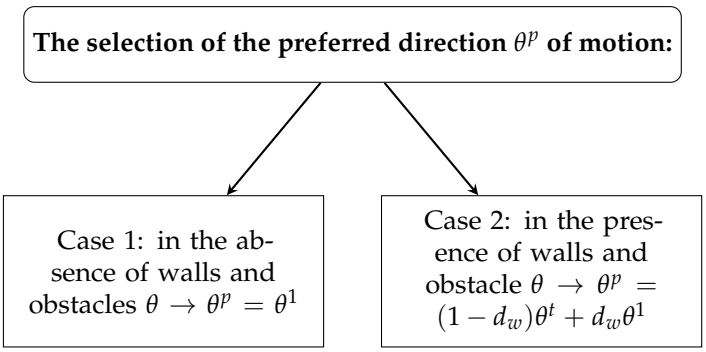


Figure 3. Selecting the preferred direction θ^p of motion.

3.2. Selection of the Preferred Velocity Modulus

Initially, we define the perceived density ρ_θ along the direction θ, which is provided according to [25] as follows:

$$\rho_\theta[\rho] = \rho + \frac{\partial_\theta \rho}{\sqrt{1 + (\partial_\theta \rho)^2}} [(1-\rho)H(\partial_\theta \rho) + \rho H(-\partial_\theta \rho)] \tag{17}$$

where

- ∂_θ denotes the derivative along the direction θ.
- $H(\cdot)$ is the Heaviside function, with $H(\cdot \geq 0) = 1$ and $H(\cdot < 0) = 0$.

Remark 9. *The perceived density $\rho_\theta[\rho]$ in a given direction θ quantifies how the density ρ of a crowd is sensed along that specific direction. It is a modified density that accounts for variations along θ, incorporating the local gradient (rate of change) of the density [25].*

After the direction of motion has been selected, the pedestrian adjusts his/her speed. Two situations can be distinguished:

- Referring to [26], if the pedestrian's speed is greater than or equal to the mean speed, then the pedestrian either maintains their speed or decelerates to a speed v_d, which is lower as the density increases. It is assumed that the probability of deceleration, denoted by p_d, increases with the environmental conditions and the overcrowding of the space [26].
  Accordingly, if $||\boldsymbol{\xi}|| < v$, then the preferred speed v^p reads as follows:

$$v^p = \begin{cases} v_d & \text{with probability } p_d \\ v & \text{else} \end{cases} \tag{18}$$

  where

$$v_d = (1 - \rho_\theta[\rho])||\boldsymbol{\xi}||, \quad p_d = \rho_\theta[\rho](1 - \lambda\alpha); \tag{19}$$

  here, the constant $\lambda < 1$ has been inserted to take into consideration the probability of deceleration being non-zero even if $\alpha = 1$ [26].
  The main features of the selection of the preferred direction θ^p of motion are summarized in Figure 4.

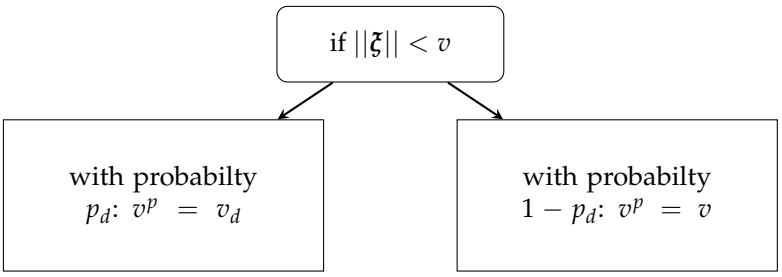


Figure 4. Selection of the preferred speed v^p.

- Referring to [26], if the pedestrian's speed is lower than the mean speed, the pedestrian either maintains their speed or accelerates to a speed v_a which is as much higher as the density becomes lower, the higher is the gap between the mean speed and the preferred speed and the goodness are the environmental conditions. It is assumed that the probability of acceleration, denoted by p_a, decreases with the badness of the environmental conditions and the overcrowding of the space [26].
  Accordingly, if $||\boldsymbol{\xi}|| \geq v$, the preferred speed v^p reads as follows:

$$v^p = \begin{cases} v_a & \text{with probability } p_a \\ v & \text{else} \end{cases} \tag{20}$$

  where

$$v_a = ||\boldsymbol{\xi}|| + \lambda(1 - \rho_\theta[\rho])(\lambda - ||\boldsymbol{\xi}||), \quad p_a = \lambda(1 - \rho_\theta[\rho]). \tag{21}$$

In Equations (19) and (21), $\rho_\theta[\rho]$ is the perceived density provided by Equation (17) along the preferred walking direction θ defined in Equation (15).

The main features of the selection of the preferred velocity modulus v^p are summarized in Figure 5.

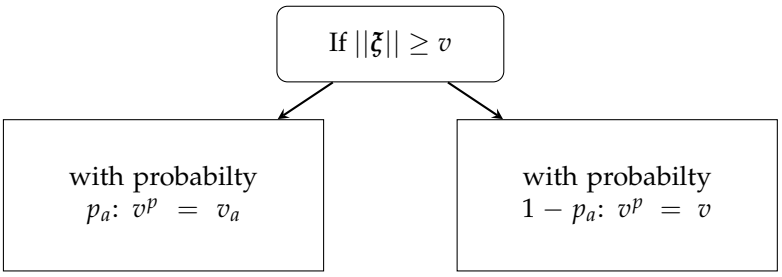


Figure 5. Selection of the preferred speed v^p.

Remark 10. *In [25], walkers interact with all others in their visibility domain; however, in the present paper we assume that their mutual interactions depend only on the density and mean velocity [26].*

The governing equation

The relaxation parameter τ defined in (7) and the equilibrium density $\mathcal{S}_{\text{eq}}$ defined in (8) are replaced by their respective expressions, and the model partial derivative equation (PDE) (6) with initial conditions becomes

$$\begin{cases} \partial_t f(t,\boldsymbol{x},\boldsymbol{v}) + \boldsymbol{v} \cdot \nabla_{\boldsymbol{x}} f(t,\boldsymbol{x},\boldsymbol{v}) = \frac{1}{\tau_0}\left(\frac{\rho(t,\boldsymbol{x})}{2\pi v_m^2} \exp\left(-\frac{1}{2}\frac{\|\boldsymbol{v}-\boldsymbol{v}^p\|^2}{v_m^2}\right) - f(t,\boldsymbol{x},\boldsymbol{v})\right), \\ f(0,\boldsymbol{x},\boldsymbol{v}) = f_0(\boldsymbol{x},\boldsymbol{v}), \quad \boldsymbol{x} \in \Omega, \quad \boldsymbol{v} \in \mathcal{V}, \end{cases} \tag{22}$$

where $\boldsymbol{v^p} = v^p(\cos\theta^p, \sin\theta^p)$ and θ^p, as provided by Equations (15) and (16), and v^p is defined by Equations (18)–(21).

4. Results and Numerical Simulations

Kinetic crowd models have been solved numerically using both deterministic and stochastic methods [1]. Deterministic methods include the finite difference method [17,18,21], the semi-Lagrangian method [33], and the finite volume method [19,22], while stochastic methods such as the Monte Carlo method have also been employed [23,25–27]. In this paper, a Monte Carlo particle scheme is adopted and further developed. Compared with deterministic solution methods, this stochastic method presents several appealing characteristics that make it one of the most favored and widely employed simulation techniques for solving kinetic crowd models:

- Effortless handling of complex geometries [25].
- High-performance computing optimization to ensure that the computational time is less than the real simulated time [1].
- Efficient handling of intricate interaction rules among pedestrians [26].
- Ability to take the level of stress of the crowd into account [23].

Simulations were conducted to demonstrate the model's capability to depict emergent behaviors observed in reality [6]. Specifically, in this study we assessed the ability of the proposed model to capture certain collective behaviors observed experimentally, such as self-organization leading to increased evacuation times under stressful conditions. Additionally, we examined whether the dynamics exhibit segregation and how high-density concentration zones evolve over time and space in the case of bidirectional flow in a straight corridor.

In this context, we employed the Monte Carlo method to analyze two critical scenarios in crowd dynamics:

1. Evacuation from a room: we investigated the impact of anxiety conditions on evacuation time, highlighting how different levels of anxiety influence crowd movement and safety during emergencies, which were not addressed in [33].

2. Counter-flow dynamics: We studied counter-flow scenarios, where two groups of pedestrians move in opposite directions, such as in a narrow corridor. The objective of this simulation was to observe whether the dynamics exhibit segregation and how high-density concentration zones evolve in time and space as in [23], which were not covered in [33].

The rest of this section is devoted to the numerical method and results. We begin by briefly describing the principle of the numerical method, which is based on the Monte Carlo method. For additional details on this method and its applications, see the standard book [36] and the references therein. Then, numerical results are presented to evaluate the ability of the proposed model to simulate crowd evacuation during stressful situations and pedestrian bidirectional flow in a straight corridor.

4.1. Numerical Method

Realistic numerical simulations were implemented using a probabilistic numerical scheme which arises from the direct simulation Monte Carlo (DSMC) method. As in typical Monte Carlo particle methods, the initial step involves a splitting technique that separately handles the transport and interaction parts of Equation (22) [36].

4.1.1. Splitting Approach

Considering the proposed mathematical model on an interval of time $[0, T]$ defined by

$$\begin{cases} \partial_t f(t,\boldsymbol{x},\boldsymbol{v}) + \boldsymbol{v}\cdot\nabla_{\boldsymbol{x}} f(t,\boldsymbol{x},\boldsymbol{v}) = \frac{1}{\tau_0}\left(\frac{\rho(t,\boldsymbol{x})}{2\pi v_m^2}\exp\left(-\frac{1}{2}\frac{\|\boldsymbol{v}-\boldsymbol{v}^p\|^2}{v_m^2}\right) - f(t,\boldsymbol{x},\boldsymbol{v})\right), \\ f(0,\boldsymbol{x},\boldsymbol{v}) = f_0(\boldsymbol{x},\boldsymbol{v}), \quad \boldsymbol{x}\in\Omega, \quad \boldsymbol{v}\in\mathcal{V}. \end{cases} \tag{23}$$

we partition domain in time the interval [0, T] using a mesh $t_0, ..., t_N$. We assume a uniform partition in time, meaning that the difference between two consecutive time points will be Δt.

For the sake of simplicity, the splitting method consists of solving the two following problems P_A and P_B separately and consecutively in a time interval $[0, \Delta t]$. First, we integrate the space homogeneous equation for all $x \in \Omega$,

$$P_A : \begin{cases} \partial_t f^*(t,\boldsymbol{x},\boldsymbol{v}) = \frac{1}{\tau_0}\left(\frac{\rho^*(t,\boldsymbol{x})}{2\pi v_m^2}\exp\left(-\frac{1}{2}\frac{\|\boldsymbol{v}-\boldsymbol{v}^p\|^2}{v_m^2}\right) - f^*(t,\boldsymbol{x},\boldsymbol{v})\right), \quad t\in[0,\Delta t], \\ f^*(0,\boldsymbol{x},\boldsymbol{v}) = f_0(\boldsymbol{x},\boldsymbol{v}), \quad \boldsymbol{x}\in\Omega, \quad \boldsymbol{v}\in\mathcal{V}, \end{cases} \tag{24}$$

for a time step Δt (interaction step) to obtain $f^*(\Delta t, \boldsymbol{x}, \boldsymbol{v}) = P_A^{\Delta t}(f_0(\boldsymbol{x}, \boldsymbol{v}))$.

Then, we solve the transport equation using the output of the previous step as initial condition

$$P_B : \begin{cases} \partial_t f(t,\boldsymbol{x},\boldsymbol{v}) + \boldsymbol{v}\cdot\nabla_x f = 0, \quad t\in[0,\Delta t], \\ f(0,\boldsymbol{x},\boldsymbol{v}) = f^*(\Delta t,\boldsymbol{x},\boldsymbol{v}), \quad \boldsymbol{x}\in\Omega, \quad \boldsymbol{v}\in\mathcal{V}, \end{cases} \tag{25}$$

for a time step Δt (transport step) to obtain $f(\Delta t, \boldsymbol{x}, \boldsymbol{v}) = P_B^{\Delta t}(f^*(\Delta t, \boldsymbol{x}, \boldsymbol{v}))$.

After this splitting, the major numerical difficulties are in the problem P_A, corresponding to the collision step, while the problem P_B corresponds to simple free flow of particles.

The transport Equation (25) can be solved exactly, and corresponds to free motion of particles. Therefore, if $\left(\boldsymbol{x}_j^0, \boldsymbol{v}_j^0\right), j = 1, \ldots, M$ are the initial particles' position and velocity vectors in $\mathbb{R}^2 \times \mathbb{R}^2$, during the transport in a time interval Δt we have the position vectors update

$$\boldsymbol{x}_j = \boldsymbol{x}_j^0 + \boldsymbol{v}_j^0 \Delta t. \tag{26}$$

4.1.2. A Nanbu-like Method

The different Monte Carlo methods are characterized by the different approaches used to approximate the interaction operator [36]. In the present paper, the solution in one time step Δt of interaction Equation (24) is solved using a Nanbu-like particle scheme.

Let $f^0(\boldsymbol{x}, \boldsymbol{v})$ be an approximation of $f(0, \boldsymbol{x}, \boldsymbol{v})$. The forward Euler scheme applied to Equation (24) is written as

$$f_1^*(\boldsymbol{x}, \boldsymbol{v}) = \left(1 - \frac{\Delta t}{\tau_0}\right) f_0(\boldsymbol{x}, \boldsymbol{v}) + \frac{\Delta t}{\tau_0} \left(\frac{\rho^*(0, \boldsymbol{x})}{2\pi v_m^2} \exp\left(-\frac{1}{2} \frac{\|\boldsymbol{v} - \boldsymbol{v}^p\|^2}{v_m^2} \right) \right), \tag{27}$$

where $f_1^*(\boldsymbol{x}, \boldsymbol{v})$ is the approximation of $f^*(\Delta t, \boldsymbol{x}, \boldsymbol{v})$.

Clearly, if $f_0(\boldsymbol{x}, \boldsymbol{v})$ is a probability density, then $\frac{\rho^*(0,\boldsymbol{x})}{2\pi v_m^2} \exp\left(-\frac{1}{2} \frac{\|\boldsymbol{v}-\boldsymbol{v}^p\|^2}{v_m^2} \right)$ is a probability density. Under the restriction $\frac{\Delta t}{\tau_0} \leq 1$, then $f_1^*(\boldsymbol{x}, \boldsymbol{v})$ is also a probability density, as it is a convex combination of probability densities. A Monte Carlo method is then obtained by direct sampling of Equation (27).

We can readily derive Algorithm 1 in order to generate samples from the probability density $f_1^*(\boldsymbol{x}, \boldsymbol{v})$ in the following way.

Algorithm 1: Nanbu-like algorithm.

1 Fix $1 <= M$, given a set of samples $(\boldsymbol{x}_1^0, \boldsymbol{v}_1^0), \ldots, (\boldsymbol{x}_M^0, \boldsymbol{v}_M^0)$ from the initial distribution density $f_0(\boldsymbol{x}, \boldsymbol{v})$.
2 **for** $j = 1, \ldots, M$ **do**
3 $\quad \boldsymbol{x}_j^{\Delta t} = \boldsymbol{x}_j^0 + \boldsymbol{v}_j^0 \Delta t$.
4 The space domain to be simulated is covered by a mesh of cells.
5 In each space cell, given a sample $\left(\boldsymbol{x}_j^{\Delta t}, \boldsymbol{v}_j^0\right)$.
6 With probability $\frac{\Delta t}{\tau_0}$ do the following:

- Replace $\boldsymbol{v}_j^0$ with $\boldsymbol{v}_j^{\Delta t}$ by sampling them from the probability density $\frac{\rho^*(0,\boldsymbol{x}_j)}{2\pi v_m^2} \exp\left(-\frac{1}{2} \frac{\left\|\boldsymbol{v}_j-\boldsymbol{v}^p\right\|^2}{v_m^2} \right)$.

Otherwise

- Set $\boldsymbol{v}_j^{\Delta t} = \boldsymbol{v}_j^0$.

4.2. Numerical Results

This part includes two sample simulations. The first simulation involves the evacuation of a room with an exit, while the second deals with two groups moving in opposite directions.

The following parameters have been selected for all simulations:

- The quality of the environment $\alpha = 1$.
- $V_m = 2$ m/s.
- $\rho_{\max} = 7$ pedestrians/m^2 [44].
- The relaxation parameter $\tau = 0.5$.

Remark 11. *The choice of ($N \leq 100$ pedestrians) in the following simulations was made to validate the model's qualitative behavior while ensuring computational feasibility.*

4.2.1. Influence of the Anxiety Conditions on Evacuation Time

Our goal is to examine how the evacuation time is impacted by the level of anxiety, which is defined by the parameter β that influences the attraction towards the mean stream relative to the tendency towards the target.

We consider a group of 26 people with an anxiety level of $\beta = 0.5$ moving inside a square room with a side length 10 m and one exit door of size 1.5 m located on the middle of the right side, as shown in Figure 6.

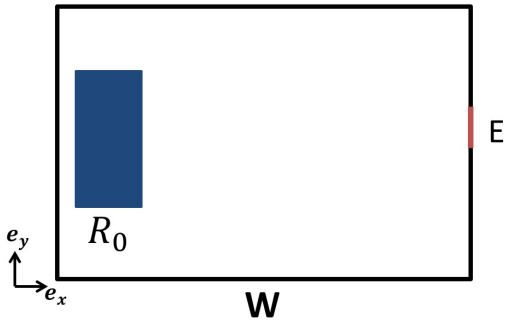
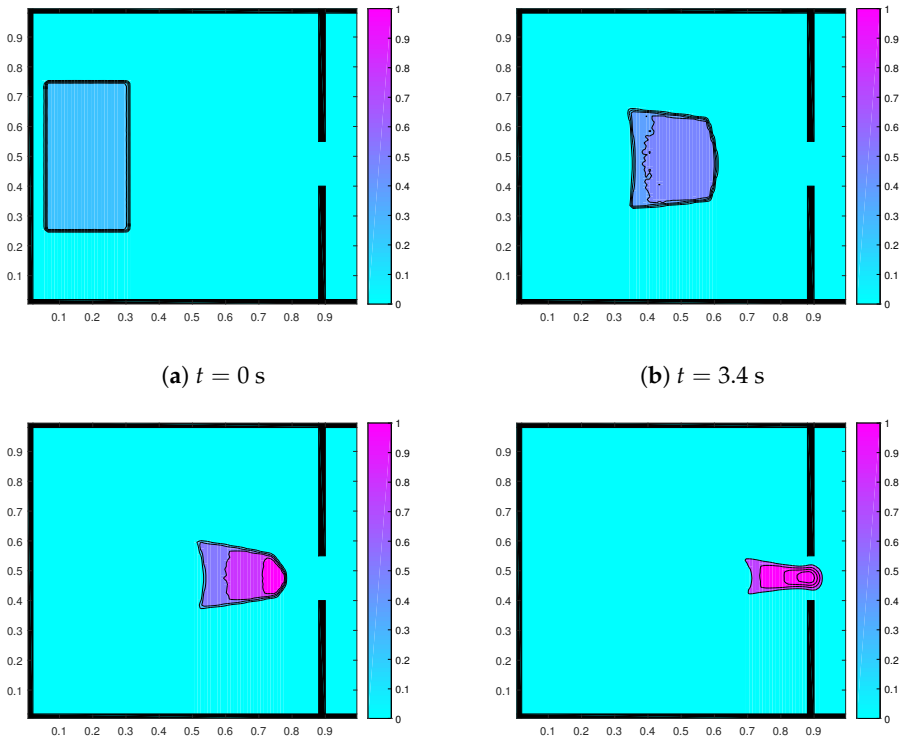


Figure 6. Illustration of the walking domain: W, wall; R_0, rectangular region; E, exit.

First, our aim is to simulate the evacuation process of individuals who are initially uniformly distributed in a rectangular region of size 2.5 m $\times$ 5 m with a density $\rho = 0.3$. The results of our simulation model at four successive times during the evacuation process are illustrated in Figure 7a–d. Figure 7 illustrates the evacuation process, showing the tendency of pedestrians to move toward the exit.



(**a**) $t = 0$ s (**b**) $t = 3.4$ s

(**c**) $t = 5.3$ s (**d**) $t = 7.2$ s

Figure 7. Density contour plot ρ of crowds for (**a**) $t = 0$ s, (**b**) $t = 3.4$ s, (**c**) $t = 5.3$ s, and (**d**) $t = 7.2$ s.

As in [25], we investigate the dependence of evacuation time on the anxiety level β by starting with another group of 52 pedestrians located inside the same room and initially uniformly distributed in the same rectangular region with a density of $\rho = 0.6$. We vary

the value of β in the range of $[0, 1]$ and collect the evacuation time data for both initial conditions. The results are presented in Figure 8.

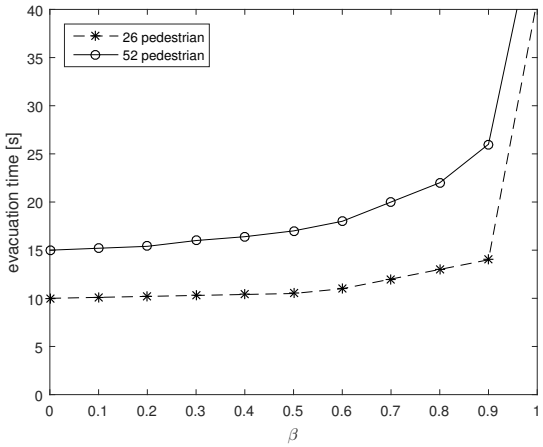


Figure 8. Evacuation time for different numbers of pedestrians versus β.

Figure 8 shows that the evacuation time increases as the anxiety level β increases for both initial conditions. A possible interpretation of this result is that the tendency to follow other pedestrians leads to overcrowding, which in turn reduces the pedestrians' speed. Moreover, the movement of pedestrians becomes more irregular as β approaches 1, which is because the stimulus to reach the target is reduced.

When compared to [25], our numerical results, lead to the same conclusion, namely, that increasing stress drives the crowd toward irrational behaviors which can induce unsafe conditions. This consistency in findings further validates our model's ability to replicate the impact of anxiety on crowd dynamics and its agreement with established results in the literature.

These simulations can aid in crisis management by demonstrating that the model accurately describes crowd dynamics as well as by showing how evacuation time increases under anxiety conditions [25].

4.2.2. Flows of Crowds Moving in Opposite Directions

This section focuses on a simulation of bidirectional flow with two crowds walking in opposite directions [23].

As in [23], the main goal of this simulation is to observe whether the dynamics exhibit segregation and how high-density concentration zones evolve in time and space.

The initial conditions of the crowd and the geometry of the venue are illustrated in Figure 9. At time $t = 0$ s, we consider a group of people moving along a rectangular venue of $L_x \times L_y = 20$ m $\times$ 5 m and another group walking in the immediately opposite directions. The group on the left (blue) is composed of 14 pedestrians uniformly distributed in a rectangular area of 4 m $\times$ 1 m, while the group on the right (red) contains 28 people uniformly distributed in a rectangular area of 4 m $\times$ 2 m.

It is assumed that the anxiety level does not propagate through the crowd and that the two groups maintain constant anxiety levels during the simulation. Specifically, the anxiety level of the group on the right is high at $\beta = 0.8$, while the anxiety level of the group on the left is normal at $\beta = 0.2$. As a result, the crowd on the right forces against the crowd on the left. This scenario could occur if the group on the right encountered a perilous situation and decided to reverse the direction of motion to avoid being killed or seriously injured [23].

The results of the proposed model associated with the case study under consideration are illustrated in Figure 10 for different times, which respectively show the gradual

formation of high-concentration zones of density and the continuation of a high level of concentration even when both groups have totally crossed one another.

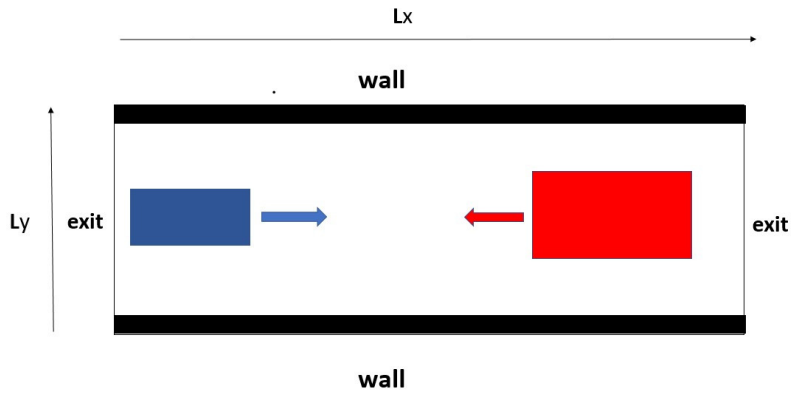
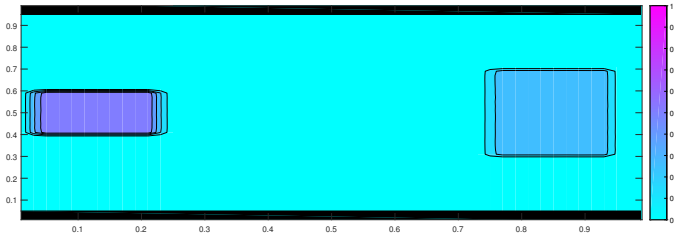
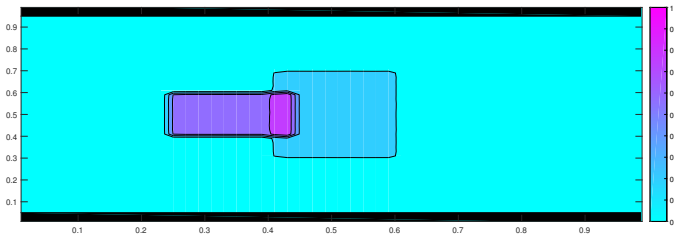


Figure 9. Two groups (red and blue) walking in opposite directions in a straight corridor of dimensions $L_x \times L_y$.

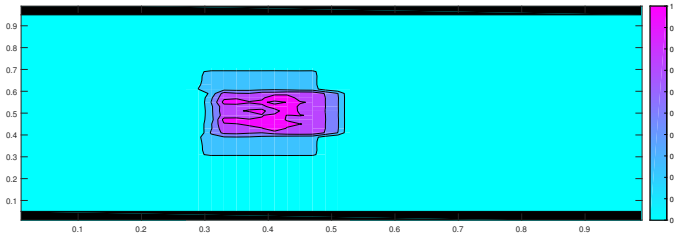
Further details of the density patterns reveal that both groups start with an initial density close to 3 pedestrians/m^2, which can be considered high but not critical [44]. However, the interaction between these two groups induces zones with a density concentration close to 7 pedestrians/m^2, which is a critical density level [44] that can lead to loss of safety conditions [23].



(**a**) $t = 0$ s

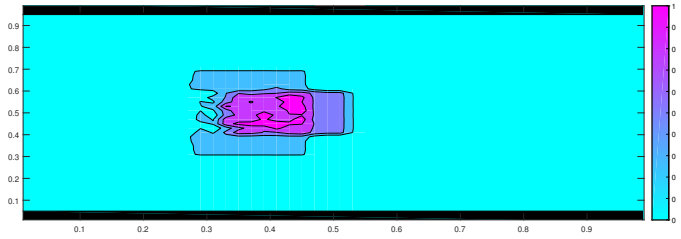


(**b**) $t = 3.7$ s

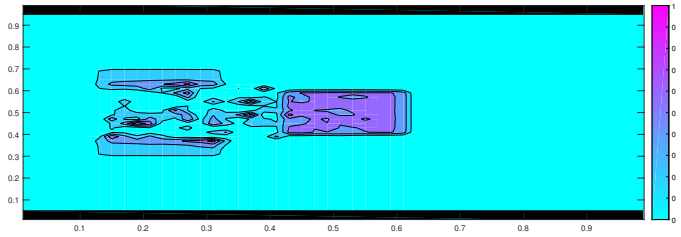


(**c**) $t = 4.9$ s

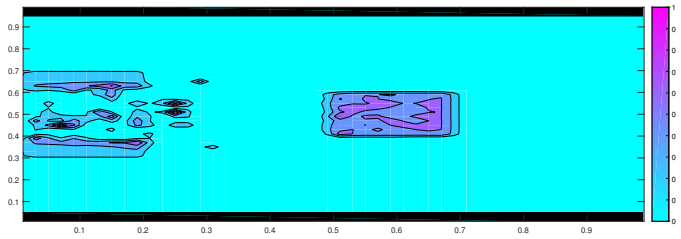
Figure 10. *Cont.*



(**d**) $t = 5.2$ s



(**e**) $t = 6.6$ s



(**f**) $t = 7.8$ s

Figure 10. Density contour plot ρ of crowds for (**a**) $t = 0$ s, (**b**) $t = 3.7$ s, (**c**) $t = 4.9$ s, (**d**) $t = 5.2$ s, (**e**) $t = 6.6$ s and (**f**) $t = 7.8$ s.

5. Conclusions

In this paper, a behavioral crowd model has been developed by means of the Bhatnagar–Gross–Krook (BGK) kinetic equation framework. The proposed model describes the tendency of a crowd towards a state of equilibrium, that is, the tendency towards a comfortable situation. Our numerical simulation results show that the suggested model is able to reproduce and describe an emerging property, namely, increased evacuation time due to anxiety. Furthermore, our simulation results related to counter-flow can offer support to crisis managers tasked with mitigating risk through the visualization of high concentration zones and explanation of how the localization of high concentration zones evolves across time and space. Although this study considers two application examples, namely, the evacuation of a room and the simulation of two groups moving in opposite directions, further investigation can be conducted on other scenarios in more complex walking spaces, for example evacuations in metro or subway stations [45–47].

Author Contributions: Conceptualization, N.B., A.E.M. and A.H.; methodology, N.B.; software, N.B.; validation, N.B. and A.E.M.; writing—original draft preparation, N.B.; writing—review and editing, N.B. and A.E.M.; supervision, A.H. All authors have read and agreed to the published version of the manuscript.

Funding: This research received no external funding.

Data Availability Statement: Data are contained within the article.

Acknowledgments: The authors sincerely appreciate the reviewers for their valuable comments and suggestions, which have significantly enhanced the quality of this paper.

Conflicts of Interest: The authors declare no conflicts of interest.

References

1. Bellomo, N.; Liao, J.; Quaini, A.; Russo, L.; Siettos, C. Human behavioral crowds review, critical analysis and research perspectives. *Math. Models Methods Appl. Sci.* **2023**, *33*, 1611–1659. [CrossRef]
2. Helbing, D.; Molnár, P. Social force model for pedestrian dynamics. *Phys. Rev. E* **1995**, *51*, 4282–4286. [CrossRef] [PubMed]
3. Kirchner, A.; Schadschneider, A. Simulation of evacuation processes using a bionics-inspired cellular automaton model for pedestrian dynamics. *Phys. A Stat. Mech. Appl.* **2002**, *312*, 260–276. [CrossRef]
4. Cristiani, E.; Piccoli, B.; Tosin, A. *Multiscale Modeling of Pedestrian Dynamics*; MS&A. Modeling, Simulation and Applications; Springer: Cham, Switzerland, 2014; Volume 12.
5. Aylaj, B.; Bellomo, N.; Gibelli, L.; Reali, A. A unified multiscale vision of behavioral crowds. *Math. Models Methods Appl. Sci.* **2020**, *30*, 1–22. [CrossRef]
6. Bellomo, N.; Gibelli, L.; Quaini, A.; Reali, A. Towards a mathematical theory of behavioral human crowds. *Math. Models Methods Appl. Sci.* **2022**, *32*, 321–358. [CrossRef]
7. Bellomo, N.; Bingham, R.; Chaplain, M.A.J.; Dosi, G.; Forni, G.; Knopoff, D.A.; Lowengrub, J.; Twarock, R.; Virgillito, M.E. A multiscale model of virus pandemic: Heterogeneous interactive entities in a globally connected world. *Math. Models Methods Appl. Sci.* **2020**, *30*, 1591–1651. [CrossRef]
8. Calvo, J.; Nieto, J.; Zagour, M. Kinetic Model for Vehicular Traffic with Continuum Velocity and Mean Field Interactions. *Symmetry* **2019**, *11*, 1093. [CrossRef]
9. Burini, D.; De Lillo, S.; Gibelli, L. Collective learning modeling based on the kinetic theory of active particles. *Phys. Life Rev.* **2016**, *16*, 123–139. [CrossRef]
10. Bellomo, N.; Dolfin, M.; Liao, J. Life and self-organization on the way to artificial intelligence for collective dynamics. *Phys. Life Rev.* **2024**, *51*, 1–8. . [CrossRef]
11. Bellomo, N.; Egidi, M. From Herbert A. Simon's legacy to the evolutionary artificial world with heterogeneous collective behaviors. *Math. Models Methods Appl. Sci.* **2024**, *34*, 145–180. [CrossRef]
12. Simon, H.A. *The Science of the Artificial*, 3rd ed.; MIT Press: Boston, MA, USA, 2019.
13. Burini, D.; Chouhad, N.; Bellomo, N. Waiting for a mathematical theory of living systems from a critical review to research perspectives. *Symmetry* **2023**, *15*, 351. [CrossRef]
14. Bellomo, N.; Burini, D.; Dosi, G.; Gibelli, L.; Knopoff, D.; Outada, N.; Terna, P.; Virgillito, M.E. What is life? A perspective of the mathematical kinetic theory of active particles. *Math. Models Methods Appl. Sci.* **2021**, *31*, 1821–1866. [CrossRef]
15. Bellomo, N.; Bellouquid, A. On the modeling of crowd dynamics: Looking at the beautiful shapes of swarms. *Netw. Heterog. Media* **2011**, *6*, 383–399. [CrossRef]
16. Bellomo, N.; Bellouquid, A.; Knopoff, D. From the Microscale to Collective Crowd Dynamics. *Multiscale Model. Simul.* **2013**, *11*, 943–963. [CrossRef]
17. Agnelli, J.P.; Colasuonno, F.; Knopoff, D. A kinetic theory approach to the dynamics of crowd evacuation from bounded domains. *Math. Models Methods Appl. Sci.* **2015**, *25*, 109–129. [CrossRef]
18. Elmoussaoui, A.; Argoul, P.; El Rhabi, M.; Hakim, A. Discrete kinetic theory for 2D modeling of a moving crowd: Application to the evacuation of a non-connected bounded domain. *Comput. Math. Appl.* **2018**, *75*, 1159–1180. [CrossRef]
19. Kim, D.; Quaini, A. A kinetic theory approach to model pedestrian dynamics in bounded domains with obstacles. *Kinet. Relat. Models* **2019**, *12*, 1273–1296. [CrossRef]
20. Liao, J.; Zhou, L. A kinetic modeling of crowd evacuation with several groups in complex venues. *Math. Models Methods Appl. Sci.* **2022**, *32*, 1785–1805. [CrossRef]
21. Liao, J.; Ren, Y.; Yan, W. Kinetic modeling of a leader–follower system in crowd evacuation with collective learning. *Math. Models Methods Appl. Sci.* **2023**, *33*, 1099–1117. [CrossRef]
22. Ma, J.; Wang, M.; Li, L. A kinetic theory model of human crowds accounting for visual attention. *Simulation* **2022**, *98*, 1039–1056. [CrossRef]
23. Elaiw, A.; Al-Turki, Y. Particle Methods Simulations by Kinetic Theory Models of Human Crowds Accounting for Stress Conditions. *Symmetry* **2020**, *12*, 14. [CrossRef]
24. Elaiw, A.; Al-Turki, Y.; Alghamdi, M. A Critical Analysis of Behavioural Crowd Dynamics—From a Modelling Strategy to Kinetic Theory Methods. *Symmetry* **2019**, *11*, 851. [CrossRef]
25. Bellomo, N.; Gibelli, L. Toward a mathematical theory of behavioral-social dynamics for pedestrian crowds. *Math. Models Methods Appl. Sci.* **2015**, *25*, 2417–2437. [CrossRef]
26. Bellomo, N.; Gibelli, L.; Outada, N. On the interplay between behavioral dynamics and social interactions in human crowds. *Kinet. Relat. Models* **2019**, *12*, 397–409. [CrossRef]

27. Bakhdil, N.; El Mousaoui, A.; Hakim, A. A kinetic theory approach to model pedestrian social groups behavior in bounded domain. *Kinet. Relat. Models* **2024**, *17*, 88–106. [CrossRef]
28. Agnelli, J.P.; Buffa, B.; Knopoff, D.; Torres, G. A Spatial Kinetic Model of Crowd Evacuation Dynamics with Infectious Disease Contagion. *Bull. Math. Biol.* **2023**, *85*, 23. [CrossRef]
29. Agnelli, J.P.; Armas, C.; Knopoff, D.A. Kinetic Modeling of Social Crowds with Infectious Disease Contagion. *Preprints* **2024**, 2024112085. . [CrossRef]
30. Kim, D.; O'Connell, K.; Ott, W.; Quaini, A. A kinetic theory approach for 2D crowd dynamics with emotional contagion. *Math. Models Methods Appl. Sci.* **2021**, *31*, 1137–1162. [CrossRef]
31. Kim, D.; Quaini, A. Coupling kinetic theory approaches for pedestrian dynamics and disease contagion in a confined environment. *Math. Models Methods Appl. Sci.* **2020**, *30*, 1893–1915. [CrossRef]
32. Kim, D.; Labate, D.; Mily, K.; Quaini, A. Data Driven Learning to Enhance a Kinetic Model of Distressed Crowd Dynamics. *arXiv* **2024**, arXiv:2411.12974. [CrossRef]
33. El Mousaoui, A.; Argoul, P.; El Rhabi, M.; Hakim, A. Kinetic BGK model for a crowd: Crowd characterized by a state of equilibrium. *Appl. Math.* **2021**, *66*, 145–176. [CrossRef]
34. Dogbe, C. On the modelling of crowd dynamics by generalized kinetic models. *J. Math. Anal. Appl.* **2012**, *387*, 512–532. [CrossRef]
35. Henderson, L.F. The statistics of crowd fluids. *Nature* **1971**, *229*, 381–383. [CrossRef]
36. Pareschi, L.; Toscani, G. *Interacting Multiagent Systems: Kinetic Equations and Monte Carlo Methods*; Oxford University Press: Oxford, UK, 2014.
37. Kant, I. *Critique of the Power of Judgment*; Cambridge University Press: Cambridge, UK, 2000.
38. Schrödinger, E. *What Is Life? The Physical Aspect of the Living Cell*; Cambridge University Press: Cambridge, UK, 1944.
39. Hartwell, L.H.; Hopfield, J.J.; Leibler, S.; Murray, A.W. From molecular to modular cell biology. *Nature* **1999**, *402*, C47–C52. [CrossRef]
40. Aylaj, B.; Bellomo, N.; Gibelli, L.; Knopoff, D. *Crowd Dynamics by Kinetic Theory Modeling*; Synthesis Lectures on Mathematics & Statistics; Springer: Cham, Switzerland, 2021.
41. Bellomo, N.; Bellouquid, A.; Gibelli, L.; Outada, N. *A Quest Towards a Mathematical Theory of Living Systems*; Birkhäuser-Springer: New York, NY, USA, 2017.
42. Cercignani, C.; Illner, R.; Pulvirenti, M. *The Mathematical Theory of Diluted Gas*; Springer: Berlin/Heidelberg, Germany; New York, NY, USA, 1993.
43. Aristov, V.V. Biological systems as nonequilibrium structures described by kinetic methods. *Results Phys.* **2019**, *13*, 102232. [CrossRef]
44. Buchmüller, S.; Weidmann, U. *Parameters of Pedestrians, Pedestrian Traffic and Walking Facilities*; IVT-Report Nr. 132; Institut for Transport Planning and Systems (IVT), Swiss Federal Institute of Technology Zurich (ETHZ): Zurich, Switzerland, 2006.
45. Guo, K.; Zhang, L. Simulation-based passenger evacuation optimization in metro stations considering multi-objectives. *Autom. Const.* **2022**, *133*, 104010. [CrossRef]
46. Zhou, R.; Cui, Y.; Wang, Y.; Jiang, J. A modified social force model with different categories of pedestrians for subway station evacuation. *Tunn. Undergr. Space Technol.* **2021**, *110*, 103837. [CrossRef]
47. Lin, X.; Cheng, L.; Zhang, S.; Wang, Q. Simulating the effects of gate machines on crowd traffic based on the modified social force model. *Mathematics* **2023**, *11*, 780. [CrossRef]

Disclaimer/Publisher's Note: The statements, opinions and data contained in all publications are solely those of the individual author(s) and contributor(s) and not of MDPI and/or the editor(s). MDPI and/or the editor(s) disclaim responsibility for any injury to people or property resulting from any ideas, methods, instructions or products referred to in the content.